PROCEEDINGS, Fifteenth Workshop on Geothermal Reservoir Engineering
Stanford University, Stanford, California, January 23-25, 1990
SGP-TR-130

GEOTHERMAL PROJECT AT ST. LUCIA (W.I.) - A PRELIMINARY ASSESSMENT OF THE RESOURCE.

Rivera, R.J.*, D'Amore, F.**, Giusti, D.*, Rossi, R.*, and Tomaselli, F.***

* Aquater, S.p.A., S. Lorenzo in Campo, PS, Italy.
** Istituto Internazionale per le Ricerche Geotermiche, Pisa, Italy
*** United Nations Revolving Fund for Natural Resources Exploration

ABSTRACT

Two deep wells were drilled in St. Lucia (W.I.); one of them was productive. A brief description of the geological characteristics from both wells is included. Extensive pressure and temperature surveys were carried out during the stages of drilling and completion of both wells and during the discharge tests on the productive well. A high-temperature, permeable zone was ~~individuated~~ indicated in the Sulphur Springs area below 4382 ft.

Two production tests were carried out in order to have a preliminary assessment of the productivity of the well. Analyses of fluid samples taken from the production line under controlled pressure and temperature conditions, allowed the definition of several basic geothermal characteristics. From these measurements it was possible to see that produced fluids exhibited chemical and physical characteristics belonging to a vapor-dominated geothermal system. Produced fluids were characterized by a high gas/steam ratio (up to about 25% in weight), high H_2/H_2S ratio, and the presence of HCl in the condensed steam.

To obtain the basic characteristics of the reservoir, injection-fall-off and pressure buildup tests were conducted. Interpretation of pressure drawdown experienced during the two production tests was carried out by means of several models, obtaining good agreement. A decrease in well productivity from the initially measured value to that obtained at the end of the tests was experienced.

GENERAL BACKGROUND

The island of Saint Lucia belongs to the Windward Islands in the Lesser Antilles, it is located between Martique and ST. Vincent within 13°43' and 14°07' latitude N and 61°05' of longitude W; it is 25 miles long and up to 12 miles wide, covering a total area of about 250 square miles (Fig. 1). The island is made up almost exclusively of products of volcanic origin, emplaced by several centers scattered in various localities. Oldest rocks, outcropping in the northermost part, are represented by andesitic agglomerates with 18.3 Ma absolute age . Lower Miocene reef-type limestone had also been identified.

Evidences of volcanic activities were limited to the northern part until the end of Miocene around 5-6 Ma[1,2] when several apparata with composition ranging from basalts to andesites were emplaced in various localities scattered from North to South. During Pleistocene several medium-small size strato-volcanoes with andesitic composition were emplaced mainly in the mid-southern part of the island. Most recent activity occurred within the Qualibou depression whose geology has been described as a caldera collapse[3] .

Alternatively, other authors[4] proposed the formation of the Qualibou depression by gravity slide. The depression edges are no longer circular and are mainly controlled by a NE-SW tectonic trend; intense activity was developped inside this area with emplacement of various dacitic domes among which the two spectacular plugs of Gros Piton and Petit Piton are the most characteristic feature of the whole island, tephra was also erupted and even the last eruptive episode had an explosive character with ejection of a dacitic flow from a center near Belfond (39,050 years B.P.)[3] . The most important tectonic alignment for the development of volcanic activity is the NE-SW trend; this direction has remained active from End - Miocene to Recent . Present activity is reduced to fumaroles with emission of gas at 172°C in the Sulphur Springs area, close to the Terre Blanche dome.

Investigation of the geothermal energy potential of the Sulphur Springs area dates back to at least 1951. However, drilling did not start until 1975-76, when 7 wells were drilled. The wells ranged in depth from 116 to 725 m and were drilled in and around the Sulphur Springs area[5,6]. From these wells three were non-productive, while the tests performed on the other four showed steam entries at boreholes 4, 5 and 7 between 230 and 350 m depth. Well 3 produced a relatively small amount of dry steam at shallow depth (133 m). The gas content of the steam was generally high varying from 15% (well 3) up

to 21% (wells 4 and 7); the composition was mainly CO_2 (90%) with less H_2 (6%), H_2S (2%), N_2 (1%) and CH_4 (0.5%). Maximum measured temperature was 220°C in well 4 at a depth of 300 m, while well 6 showed in the section from 320 to 692 m a temperature gradient of 220°C/km.

In 1982, extensive geological, geophysical and geochemical surveys pointed out the existence of a high temperature geothermal system underlying the Qualibou area. To confirm the presence of this geothermal system, two deep wells (SL-1 and SL-2) were drilled during 1987-88 in the Belfond and Sulphur Springs areas, respectively[7].

RESULTS OBTAINED FROM WELL SL-1

The location of SL-1 in the Belfond area was chosen based upon important volcanological and structural evidences which supported the presence of the heat source and secondary permeability. The main units encountered during drilling are shown in Fig. 2. As shown in this figure, the well reached a total depth of 7261 ft. This well found low permeability, as evidentiated by small fluid circulation losses during drilling. However, temperature was high, with a maximum of 241°C at total depth, as determined from the extrapolation of data obtained from a temperature buildup performed. Fig. 3 shows pressure and temperature profiles (P/T) carried out after well completion and a long shut-in period. To have a better idea of the magnitud of permeability, an step-rate injection fall-off test was performed. A value of kh = 680 md.ft was calculated. An unsuccessful attempt was made to bring the well into production.

RESULTS OBTAINED FROM WELL SL-2

Well SL-2 was located close to the Sulphur Springs area in the vicinity of the British well N. 6, which showed very high geothermal gradient (220°C/ 1000 m), with the aim to intercept at a reasonable depth a producing fractured zone associated with the main active fracture trend (NNW-SSE). Fig. 2 shows the crossed stratigraphic sequence[7].

Several temperature and pressure surveys were run in the well during the stages of drilling, completion and production. Once a high temperature and permeability zone was reached during drilling, injectivity and falloff tests were conducted in order to confirm the high capacity of the fractured zone located below 4382 ft. The calculated static formation temperature at this depth was in the order of 292°C. From the injectivity test a value of kh/μ = 25266 (md.ft/cp) was calculated. After finishing this test and based upon the encouraging evidences obtained, it was decided to run a 7" slotted-liner to protect the open interval of the well, given the completion shown in Fig. 2.

After completion, a warming-up period was allowed in order to assess the thermodynamic evolution of conditions within the wellbore. Figs. 4 and 5 show a series of P/T profiles run during this period, allowing a fairly good definition of the location of most permeable zones.

During the preliminary production test, herein called horizontal discharge test, the well initially discharged gas followed by water and a mixture of water and steam. The main aim of this test was to obtain a preliminary and rough idea about the production capacity of the well and to see if any major changes in its behavior could be detected. All measurements were conducted by means of the lip pressure method with a silencer to measure the liquid flow rate[8]. This discharge test lasted for about 70 h. A summary of production data obtained from this test are shown in Table 1 and in Fig. 6. During this brief production test it was observed that the amount of separated water was low from the start and continuosly decreased with production time, until it disappeared after about 48 hr flowing time. Another interesting observation from the behaviour exhibited by the well, was that the mass of produced gas, relative to total mass produced remained fairly constant over the whole discharge period.

Short term production test

In order to have a more precise idea of the actual productivity of the well, a longer production test was performed. This test will be refered as the "short term production test". This test was carried out for about 200 hr. Fig. 7 shows the behaviour exhibited by the well during this test.

The main characteristics of the well already evidentiated during the previous discharge test were confirmed. No water production was obtained. The mass of gas produced remained fairly constant during all the test, which supported an interesting conclusion that will be discussed latter. As it can be seen from Fig. 7, a production decline for a given wellhead pressure can be detected. Fig. 6 show production data as a function of wellhead pressure obtained during both the horizontal discharge and the short-term production tests. From this figure the declination from the initial productivity of the well is more evident.

As previous stated, fluid production was mainly in the vapor phase, except for the first hours, when some liquid water was

---

* Tables and Figures are included at the end of paper.

present. For this case isotopic and chemical compositions of gas and steam are the only tools to gather useful information for a better understanding of reservoir parameters such as temperature, gas pressures, liquid saturation, gas/total water ratio and redox conditions. For this purpouse gas composition reported in Table 2., as well as isotopic fluid composition shown in Table 3. had been used.

Reservoir equilibrium temperature was calculated by means of both isotopic geothermometers and chemical equilibrium between H_2O and H_2S species. Among isotopes, equilibrium conditions between some pairs of species produced the following results[9] :

a) $D(H_2) - D(H_2O)$: equilibrium temp. 300°C
b) $^{13}D(H_2) - ^{13}D(CH_4)$: equilibrium temp. 308°C
c) $^{13}C(CO_2) - ^{13}C(CH_4)$: equilibrium temp. 400°C

Based on the results obtained, it appears that the pairs H_2-H_2O and CH_4-H_2 produce equilibrium temperatures close to that measured in the reservoir, which was of 292 °C, as previosly stated. On the other hand, the CO_2-CH_4 pair provided a temperature about 100°C higher than the measured reservoir temperature. An explanation for this might be that, at least part of the CO_2 sampled, has a much deeper origin than the tapped fluid in the reservoir, and that equilibrium with CH_4 is reached very slowly. As a confirmation to this possible deeper origen, the high negative values of the $\delta^{18}O(CO_2)$ seem to be consistent with a strong magmatic component. This value ranged from - 6.8 to - 9.7.

Equilibrium between H_2O and H_2S was considered by means of the following equation[10] :

$$\log (H_2S/H_2O) = 5.12 - 6483.5/T - 0.79 \log T - 1/6 \log P(O_2) - \log A(H_2S) \quad (1)$$

where H_2S/H_2O is the molal measured ratio between both species and $P(O_2)$ is the oxygen partial pressure. The latter can be calculated from the following equation :

$$\log P(O_2) = -3.808 - 13708.3/T - 2.075 \times 10^6/T^2 \quad (2)$$

Meanwhile A(i) for any gas species is given as follows :

$$A(i) = y + (1-y)/B(i) \quad (3)$$

As a first approximation, considering apparent steam fraction y close to unity and then neglecting the $A(H_2S)$ term, a temperature close to 310°C may be evaluated. Meanwhile, for a value of y close to 0.5, a temperature of 290°C is computed. This value is more consistent with the measured one. Further details can be found in ref. 9 High reservoir temperatures were also confirmed by means of the D'Amore and Panichi[9] empirical geothermometer, which employs the dry gas composition; the temperature obtained was 290°C.

On the other hand the contemporaneous study of all available reactive gaseous species, will enable both verification of the equilibrium temperatures previously calculated by means of other methods, and the calculation of the CO_2 pressure. In order to accomplish the latter, the basic relationships used were the dissociation reactions for H_2O and H_2S as well as the following chemical reactions:

$$CH_4 + 2H_2O = 4H_2 + CO_2 \quad (4)$$
$$CO_2 + H_2 = CO + H_2O \quad (5)$$
$$1/3Fe_3O_4 + S_2 = FeS_2 + 2/3\ O_2 \quad (6)$$

Based on suitable linear combinations, the following two relations are obtained[9] :

$$4\log(H_2/CO_2) - 1/4\log(CH_4/CO_2) - 3\log(CO/CO_2) = 3.143 - 2458.7/T + 4.0961 \log T - 4\log P(CO_2) + 4\log A(H_2) - 3\log(CO) - 1/4\log A(CH_4) - 3/4\log A(CO_2) \quad (7)$$

$$3\log(H_2S/CO_2) - \log(H_2/CO_2) = 17.25 - 10318.15/T - 0.412 \log T - 2 \log P(CO_2) + 3 \log A(H_2S) - 2\log A(CO_2) - \log A(H_2) \quad (8)$$

These two equations are not strongly y dependent and can not produce a precise evaluation of y values. This set of equations can be solved numerically for $P(CO_2)$, fixing reservoir temperature and for different values of y. Considering a reservoir temperature of 292°C, convergency is obtained with a $P(CO_2)$ = 9.9 bar for y = 0.1.

Evaluation of reservoir gas/total water ratio and effective steam fraction

At a fixed temperature the gas/total water ratio in the reservoir can be evaluated as a function of $P(CO_2)$ and y[9] :

$$-11.382 - 6183.08/T + 0.206 \log T - 3/2 \log P(CO_2) - 3/2 \log(H_2S/CO_2) = -1/2 \log(H_2/H_2O) + 1/2 \log A(H_2) - 3/2 \log A(H_2S) + 3/2 \log A(CO_2) \quad (9)$$

$$5.019 - 2240.44/T - 0.979 \log T - \log(CO/CO_2) = -\log(H_2/H_2O) - \log A(CO) + \log A(CO_2) + \log A(H_2) \quad (10)$$

These two equations are strongly y dependent. At a temperature of 292°C, $P(CO_2)$ of 10 bar, and by using the most reliable analytical gas composition given in Table 2, a value of y = 0.3 can be computed together with a value of gas/total water ratio of about 105 liters/kg at standard conditions. This y corresponds to a volumetric liquid saturation (S_l) of 0.11. The gas/total water value is smaller than that exceeding 145 liters/kg measured at the minimum wellhead pressure.

Additional indications from geochemical data

The redox conditions in the reservoir can be

expressed by calculating the value of the oxygen partial pressure (log $P(O_2)$) at a given temperature. At 292°C the redox conditions can be expressed by a value of log $P(O_2) = -36.0 \pm 0.2$, as a result of the application of two independent equilibrium reactions, using H_2/H_2O and CO/CO_2 ratios, as described elsewhere .

As previously discussed by Giggenbach et al.[13], depending on the relative amounts of N_2, Ar, and He present in geothermal gas, three different sources can be identified for these species : recent groundwater, magmatic and crustal origin. Analysis coming from gas samples from well SL-2 suggest a relative position in the system N_2-Ar-He consistent with mixing between crustal and magmatic components. It was observed that after about 70 hours of production, the N_2/Ar ratio measured in the fluid reached values in the order of 1000. This ratio excludes the possibility of having any meteoric gas component in the fluid coming from the well. On the other hand, the ^{13}C analyses of CO_2 carried out on two gas samples confirmed an intermediate gas origin in between magmatic and an origin associated with metamorphic processes of old marine sediments. Values of $\delta^{13}C$ obtained were - 2.5 and - 2.8, respectively. The measured content of tritium on the condensed steam (0.6 T.U.) indicates that there is not substantial supply of recent meteoric water of an age less then 30 years in the output from the well.

As it can be seen from Fig. 8, chloride concentration in the condensed steam increased with production time, as wellhead pressure decreased, during the production tests. This chloride was present as HCl in the condensed steam producing a strong corrosion tendency for this fluid. It was vllso observed that pH decreased as Cl^- content increased. The highest value reached was higher then 300 ppm. Laboratory analysis of condensed steam is give in Table 4.
As it is well known, HCl together with other species such as H_2S, sulphates, chloride ions, boric acid and CO_2, can be considered as a highly corrosive agent, and it has already been identified as present in other vapour-dominated systems around the world[14,15]. Therefore, future corrosion problems in the St. Lucia geothermal resource should be expected due to the presence of this chemical species. During the production tests, ferric ions in the steam were identified, giving an indication of possible down-hole corrosion. This hypothesis was confirmed by the analysis performed on scale samples collected from the orifice plates in the production line, where the main component was iron

Pressure buildup tests

Once the short production test was ended and after carrying out P/T profiles and unsuccessful attempts to take bottom-hole fluid samples, a first buildup test was performed. Although the drawdown data were recorded, intermittent clock stoppages were present during the buildup period, rendering useless this last portion of the test. Therefore, it was decided to conduct a new buildup test. The drawdown part of the test lasted for approximately 127 minutes. After this time, the well was shut-in and the buildup portion of the survey was recorded. This test lasted 1100 minutes.

The buildup test was preceeded by a variable flow rate history, since before carrying out this test several maneuvers were performed in the well, such as the vertical discharge test, the horizontal discharge test, well flowing under bleeding conditions, and finally, the short-term production test. It was suspected that pressure transients created in the reservoir by all these changes in flow rate could had not died out completely by the time the buildup test was performed. To properly account for all these transients in the interpretation of the buildup data, a technique that superpose the effect of variable flow rate before the well is shut-in was used[16] . For this purpouse, the variable flow rate history was approximated by means of a series of constant rate steps. Assuming radial flow, the interpretation model is as follows:(*)

$$P_{ws}^2 = P_i^2 - m \sum_{j=1}^{N} \frac{W_j}{W_N} \log \left(\frac{t_N - t_{j-1}\ \Delta t}{t_N - t_j\ \Delta t} \right) \quad (11)$$

$$m = 89178.5 \frac{WZ\ T\mu}{khM} \quad (12)$$

Analyzing the data by means of a log ΔP^2 vs. log Δt plot. It was determined that wellbore storage effects should die out after approximately 37 min. shut-in time. Therefore, the correct semilog straight line will develop after 37 min., as shown in Fig. 9. From this figure, the slope of the straight line and its interception with the vertical axis are as follows:

$$m = \text{slope} = -500\ (Kg/cm^2)^2/\text{cycle}$$

$$\text{intecept} = P_i^2 = 5370\ (Kg/cm^2)^2;$$

$$P_i = 73.3\ (kg/cm^2) = 72\ (bar)$$

$$\text{From eq.(2)} : kh = \frac{89178.5WZT\mu}{m\ M} \quad (13)$$

From well temperature surveys a reservoir temperature in the order of 563 °K(290 °C) was estimated. For this temperature and the pressure conditions prevailing during the test, the steam viscosity and real gas law deviation factor are $\mu = 0.021$ cp; $Z = 0.81$, respectively.

(*) Nomenclature at the end of paper

From eq. (13):

$$kh = \frac{89178.5\ WZ\mu T}{mM} = \frac{89178.5(35)(0.81)(563)(0.021)}{18(500)} = 3321\ (md.m)$$

To check this value, analysis by means of the conventional Horner method was carried out. Fig 10 shows the semilog plot required by this method. An equivalent production time of 3024 hr. was calculated. The Horner model can be written as follows:

$$P_{ws}^2 = P_i^2 - \log\left(\frac{t_p + \Delta t}{\Delta t}\right) \qquad (14)$$

From Fig. 10 the slope and the intercept of the straight line are as follows:[16]

m = slope = $-450\ (Kg/cm^2)^2$ cycle;
intercept = $P^2 = 5730\ (Kg/cm^2)^2$

$P_i = 75.7\ (Kg/cm^2) = \underline{74.2\ (bar)}$

From eq. (13):

$$kh = \frac{89178.5\ WZ\mu T}{mM} = \frac{89178.5(35)(0.81)(563)(0.021)}{450(18)} = 3690\ (md.m)$$

As it can be seen, the kh calculated by both methods agree very well. The skin factor for the well, s, can be calculated as follows :

$$s = 1.151\left(\frac{P_{1hr}^2 - P_{wf}^2}{m} - \log\frac{k}{\phi\mu c_t r_w^2} + 3.107\right) \qquad (15)$$

An average value of 0.015 for the porosity was used. The total system compressibility was calculated as $0.0179\ (Kg/cm^2)^{-1}$. By using eq. (15) a value of s = -1.1 can be calculated.

Pressure drawdown analysis during production tests

To complete the analysis of reservoir behaviour during the two production tests, analysis of pressure drawdown during both tests was performed. For this purpouse, bottom-hole flowing pressures were calculated from wellhead pressure and flow rate data by means of well-established techniques[17] . Analysis of drawdown data was performed by using both variable-rate models[18] and Type-curve matching techniques[16] . For type curve matching two models were assumed, the parallelepiped model[19] and a well intersecting a vertical fracture[16].
Analysis of drawdown during the first production period (horizontal discharge test) was not conclusive. Results of analysis of data by means of the variable-rate model is shown in Fig. 11. Although two possible straight lines could be infered from this graph, it can be seen that neither of them actually corresponds to the semilog straight line, this fact becomes evident when a log-log analysis is perform. For this purpouse the $\Delta P^2/W$ approach was used[20,21]. Fig. 12 shows a log-log graph of $\Delta P^2/W$ vs. production time. From this graph it is possible to see that total production time was too short, and although an initial trend for the data started to show, a distrubance at about 25 hr flowing time is evident. This disturbance was due to a change in the lip pressure spool used for flow rate measurements from an initial 4" to a final 8" diameter, coupled with an increase in flow rate to about double of that before the change. As it can be seen from this figure, data points started to return to the initial trend at the end of the test.

Fig. 13 shows the interpretation of the drawdown data by means of the variable-flow rate model for the short production test. As it can be seen, two straight lines can be fitted to the model, the first one extending up to 11.4 hr flowing time, and the second one starting from 15.1 hr up to the end of the test (198.8 hr). Interpretation of the data can be performed by means of the well-known multiple-rate drawdown model[16,18]:

$$Y_{oj} = m' X_{oy} + b' \qquad (16)$$

where:

$$Y_{oj} = \frac{P_i^2 - P_{wf}^2}{W_n} \qquad (17)$$

$$X_{oj} = \sum_{j=1}^{n} \frac{(W_j - W_{j-1})}{W_n} \log(t - t_{j-1}) \qquad (18)$$

$$b' = m'\left(\log\frac{k}{\phi\mu c_t r_w^2} - 3.1070 + 0.8686s\right) \qquad (19)$$

$$m' = \frac{89178.5\ Z\ T\mu}{khM} \qquad (20)$$

For the conditions prevailing during the short production test the following average values were determined: T = 503 °K, Z = 0.88, μ = 0.021 cp. Therefore, from eq. (10) the following values of kh can be determined:

a) First straight line: m' = 14.71; kh = 3134 md.m
b) Second straight line: m' = 64.36; kh = 716 md.m

As it can be seen, the value of kh obtained by means of the first straight line agrees well with that calculated by means of the buidup test.

Interpretation of data from the short production test by means of the parallelepiped model is shown in Fig. 14. This figure shows the match obtained with this model for the case when $x_e/x_f = 2$. As it can be seen, the best match was obtained with the $h_D = 7$ curve. Departures from the general trend are observed at flowing times corresponding to abrupt changes in flow rate associated with changes in either lip pressure spools or orifice plates, but as it can be observed from the figure, the well returns to the general trend sometime after the disturbance has died out. Interpretation of data was made by means of the equations provided by Cinco et al.[19] :

Dimensionless variables:

$$P_D = 1.291\times10^{-2}\,\frac{M\sqrt{k_x k_y}\,h\,(p_i^2-p_{wf}^2)}{ZT\mu W} \qquad (21)$$

$$t_{Dxf} = 0.3604\,\frac{k_x t}{\phi\mu c_t x_f^2} \qquad (22)$$

$$x_D = \frac{x}{x_f};\quad y_D = \frac{y}{x_f}\sqrt{\frac{k_x}{k_y}},$$

$$x_D = \frac{z}{x_f}\sqrt{\frac{k_x}{k_y}} \qquad (23)$$

$$x_{De} = \frac{x_e}{x_f};\quad y_{De} = \frac{y_e}{x_f}\sqrt{\frac{k_x}{k_y}} \qquad (24)$$

$$h_{fD} = \frac{h_f}{x_f}\sqrt{\frac{k_x}{k_z}} \text{ and } z_{fD} = \frac{z_f}{x_f}\sqrt{\frac{k_x}{k_z}} \qquad (25)$$

$$h_D = \frac{h}{x_f}\sqrt{\frac{k_x}{k_z}} \qquad (26)$$

From Fig. 14, the match point is as follows:

For $P_i^2 - P_{wf}^2/W = 10(kg/cm^2)^2/(ton/h)$;

$P_D/h_D = 0.188$

For t = 10 h ; $t_{Dxf} = 1.42$

$x_e/x_f = 2$; $h_D = 7$

By using these values, the following results are obtained:

$$P_D = (P_D/h_D)\cdot h_D = (0.188)(7) = 1.316$$

Combining eqs. (21) and (26) and using the same average values for T, Z, and μ as before:

$$(k_x k_y)^{1/2} x_f (k_z/k_x)^{1/2} = \frac{P_D Z T \mu}{0.01291 M h_D} = \frac{(1.316)(0.88)(504)(0.021)}{(0.01291)(18)(7)} = 0.7535$$

$$x_f (k_y k_z)^{1/2} = 0.7535 \text{ (darcy.m)}$$

From eq. (22)

$$k_x/x_f^2 = \frac{t_{Dxf}\phi\mu c_t}{0.3604\,t} = \frac{(1.42)(0.015)(0.021)(0.0179)}{0.3604\,(10)} =$$

$$= 2.88\times10^{-5} \text{ (Darcy/m}^2\text{)}$$

Since $((k_z k_y)^{1/2} x_f)^2 (k_x/x_f^2) = k_x k_y k_z$, by using the values calculated before,

$$k_x k_y k_z = (0.7535)^2 (2.88\times10^{-5}) =$$

$$= 1.638\times10^{-5} \text{ (darcy)}^3$$

$$(k_x k_y k_z)^{1/3} = 0.0254 \text{ (darcy)}$$

In order to get a rough estimation of the permeability, let's assume $k_x = k_y = k_z = k$. From the values calculated before, the following results are obtained:

$(k_x k_y k_z)^{1/3} = k = 0.0234$ (darcy) = 25.4 md

$x_f (k_y k_z)^{1/2} = x_f k = 0.7535$; $x_f = \frac{0.7535}{0.0254} = 29.7$ m

$h = h_D x_f (k_z/k_x)^{1/2} = h_D x_f = (7)(29.7) = 208$ m;

kh = (25.4) (208) =5280m.

As it can be seen, this kh value is higher than that obtained with the conventional methods described before, but it can still be considered within the same range.

Matching of data from the same test was also performed by means of the type curve for a vertically fractured well. For this purpouse, the Uniform-Flux fracture curve presented by Gringarten et al.[16] as used. Results from this matching are shown in Fig. 15. As it can be seen from this figure, a good match with the curve for $x_e/x_f = 10$ was also obtained. The match point is as follows:

For $P_i^2 - P_{wf}^2/W = 100\ ((kg/cm^2)^2/(ton/h))$;

$P_D = 5.7$

For t = 1 h; $t_{Dxf} = 1.95$; $x_e/x_f = 10$

For this case, dimensionless variables are defined as follows:

$$P_D = \frac{M\ k\ h\ (P_i^2 - P_{wf}^2)}{774.59\ W\mu\ Z\ T} \qquad (27)$$

$$t_{Dxf} = \frac{3.48 \times 10^{-4}\ kt}{\phi\mu\ c_t\ x_f^2} \qquad (28)$$

$$x_D = \frac{x}{x_f},\ y_D = \frac{y}{x_f} \qquad (29)$$

From eq. (27) and by using the same average parameters mentioned before, as well as the values obtained from the match point, the following results are obtained:

$$kh = 77459\ \frac{Z\ T\mu}{M}\ \left(\frac{P_D}{(P_i^2-P_{wf}^2)/W}\right) =$$

$$\frac{77459(0.021)(0.88)(504)}{18}\ \left(\frac{5.7}{100}\right) = 2285\ md.m$$

From eq. (28):

$$x_f^2 h = \frac{3.48 \times 10^{-4}}{\phi\mu\ c_t}\ \left(\frac{t}{t_{Dxf}}\right) =$$

$$= \frac{0.0348(2285)}{(0.015)(0.021)(0.0179)}\ \left(\frac{1}{1.95}\right) = 72321\ m^3$$

As it can be seen, the value of kh calculated by means of the vertically fractured well model can also be considered as consistant with the value obtained from the application of the other models used. A summary of results obtained from the application of all models considered in this paper is included in Table 5.

CONCEPTUAL MODEL OF THE GEOTHERMAL SYSTEM

Drilling of wells SL-1 and SL-2 provided new stratigraphical data useful for a better definition of the geological model, which, integrated with all other data available, allowed the updating of the conceptual model of the geothermal field, which is shown in Fig. 16. This model can be summarized as follows:

1) Heat source.
The presence of a shallow magma chamber can be inferred on the basis of several volcano-tectonic evidences and supported by microseismic studies revealing the presence of at least one significant fluid body under the Sulphur Springs area. The volume of magma emplaced by the intra-depression activity seems to be relatively small and appears to be concentrated in the Sulphur Springs - Terre Blanche area. The magma body is enough (due to its shallow location) to produce an important heat anomaly around the Sulphur Springs area, as shown by well SL-1, where a geothermal gradient of about 4 times the normal gradient was found in the area of Belfond, while well SL-2 discovered a high-conductive type of thermal gradient in the first 1000 m, in the order of about 7 times the normal gradient (0. 067°C/ft).

2) Cap rock .
The most common volcanic feature of the whole Qualibou area is the presence of lavic domes. These apparata were originally permeable and represent a possible recharge zone, drilling of well SL-1 showed a good example of volcanic dome permeability; however, in zones where hydrothermal activity was particularly active, deposition of secondary minerals produced sealing of the formations (e.g. Terre Blanche dome). As drilling of SL-1 and SL-2 emphasized, volcanic agglomerates were originally a poorly permeable formation which became impervious by hydrothermal mineral deposition. This phenomenon acts also on the other basic lava flows sequences crossed in SL-1, making them impermeable.

3) Geothermal reservoir.
Considering that the available data are coming from only one well (SL-2), it was not possible to completely define the physical and thermodynamic characteristics of the reservoir, but only of the area adjacent to the well itself. A geothermal reservoir in an igneous environment, such as that of St. Lucia, is generally characterized by highly fractured formations. Well SL-2 reached slightly fractured zones below 2950 to 3300 ft, apparently saturated with gas-rich fluids; hence, a more important fractured zone was evident below 4100 ft, with maximum fracturing from 4382 ft down to bottom-hole (4636 ft). This part of the reservoir is characterized by high permeability, typical of a fractured system.

4) Recharge system.
The produced fluid is represented by superheated steam with high gas content, most probably already present in the fractures (not caused by flash phenomena during the production). It was impossible to collect representative brine samples, which are hypothezed in the lowest part of the reservoir, and to obtain direct information on their chemical characteristics in order to define the recharge system.

CONCLUSIONS

Based upon all studies and measurements performed on the two wells drilled in St. Lucia, the following conclusions can be withdrawn:

1. The stratigraphy of the wells pointed out different goe-volcanological frames: well SL-1 is characterized, beneath the Belfond dacitic dome, by the presence of a basaltic apparatus and then by a series of generally reworked lavic products with composition variable from basic to intermediate. Meanwhile, SL-2 shows, beneath the Terre Blanche dacitic dome, a volcanic agglomerate with mainly dacitic lithics and then an old dome, always with dacitic composition.

2. Well SL-2 tapped a vapour-dominated geothermal resource having high gas/steam and H_2/H_2S ratios. Condensed steam showed the presence of HCl that increased with production time, reaching a concentration higher than 300 ppm. This fact suggests the presence of a highly concentrated boiling brine at some depth in the reservoir that started boiling shortly after production began. The presence of this chemical species is an indication of future corrosion problems in those places where steam condensates.

3. Calculated reservoir temperature from bottom-hole temperature measurements was 292°C. Calculations performed using isotopic geothermometers and chemical equilibrium relationships between several gaseous species, produced reservoir equilibrium temperatures that were within the same range.

4. Produced fluids from well SL-2 exhibited an important contribution to total mass produced coming from the deeper aquifer. Contribution from shallower colder aquifers could only be identified during the first part of the horizontal discharge test, when a small amount of water was present.

5. The N_2-Ar-He content in produced fluids indicates a mixing between crustal and magmatic components. On the same line, the low measured content of Tritium indicates that there is no substantial supply of recent meteoric water of an age less than 30 years at the output of the well.

6. Computed partial pressure of CO_2 species at equilibrium conditions is in the order of 10 bar, while the effective steam fraction is close to 0.3

7. A decrease in well productivity was detected from measurements taken during the two production tests. At a wellhead pressure of 15 bar, output decreased from an intial value of about 62 ton/h, measured during the horizontal discharge test, to about 33 ton/h at the end of the short term production test. This productivity decrease corresponds mainly to a decrease in average reservoir pressure.

8. Based upon interpretation of data from well tests performed by means of several models, it can be concluded that well SL-2 has tapped a naturally fractured, double-porosity system, whose kh is in between 3000 and 5000 md.m, with a skin factor between -1 and -4.

9. The geothermal reservoir behaved as a limited vapor-dominated system with a limited recharge. The possibility of having a large initial gas cap present in the system is excluded, since the mass of gas produced remained fairly constant, even under different wellhead pressure conditions.

10. Longer production tests as well as further fluid sampling and analysis should be performed in order to confirm the preliminary results included in this paper.

NOMENCLATURE

$B(i)$	=	Gas "i" Molal distribution coefficient.
b'	=	intercept on variable-rate plot
c_t	=	total system isothermal compressibility, (kg/cm^2)
h	=	formation thickness, m
h_f	=	formation height, m
k	=	permeability, md
$(k)_{x,y,z}$	=	permeability in x,y,z direction, darcy
M	=	molecular weight, gr/gr mole
m	=	slope of semilog straight line, $((kg/cm^2)^2/cycle)$
m'	=	slope of data for a multirate test, $((kg/cm^2)^2/cycle$ ton/h)
P	=	pressure, kg/cm^2
r	=	radius, m
s	=	skin factor
T	=	reservoir temperature, °K
t	=	time, hrs
t_p	=	equivalent production time, hrs
X	=	multirate plot absisa

x = distance in x-direction, m
x_f = half-fracture length, m
x_e = boundary location in x-direction, m
y = distance in y-direction, m
y^* = vapor fraction with respect to total water in the reservoir
y_e = boundary location in y-direction, m
Z = gas deviation factor, dimensionless
z = distance in z-direction, m
z_f = elevation of midpoint of fracture, m

Subscripts

D = dimensionless
e = external
f = fracture
i = initial
l = liquid
Oj = refers to multi-rate coordinate
w = well
wf = flowing bottom-hole conditions
1hr = refers to 1 hr conditions

Greek symbols

μ = viscosity, cp
ϕ = porosity, fraction

REFERENCES

1. BRIDEN, J.C., REX, D.C., FALLAR, A.M. and TOMBLIN, J.F.: "K/Ar geochronology and palaeomagnetism of volcanic rocks in the Lesser Antilles island arc". Phil. Trans. Roy. Soc., vol. A291: (1979) pp. 485-528.

2. AQUATER: "Exploration of St. Lucia Geothermal Resources", General Report Government of St. Lucia, St. Lucia, W.I.. Unpublished report. (1982).

3. TOMBLIN, J.: "The volcanic history and petrology of the Soufriere region, St. Lucia"; Ph. D. Thesis, University of Oxford (1964).

4. WRIGHT, J.V., ROOBOL, M.J., SMITH, A.L., SPARTKS, R.S.J., BRAZIER, S.A., ROSE, W.I. Jr., and SIGURDSSON, H.: "Late Quaternary explosive silicic volcanism on St. Lucia, West Indies". Geol. Mag., vol. 121, (1984), pp. 1-15.

5. MERZ and McLELLAN: "Geothermal prospect at Soufrier" Results of exploratory holes 1-5 and 6 and 7". Government of St. Lucia, unpublished reports (1976 and 1977).

6. WILLIAMSON, K.H.: "A model for the Sulphur Springs Geothermal Field,St. Lucia"; Geothermics, vol. 8, (1979), pp. 75-83.

7. AQUATER: "Geothermal Exploration Drilling Project, Saint Lucia (W.I.), Final Report", (Dec., 1988). Unpublished report.

8. JAMES, R.; "Metering of steam-water two-phase flow by sharp edged orifices", Proc. Inst. Mech. Eng. Vol 180, Pt. 1 No. 23, (1965-1966) 549-572.

9. D'AMORE, F., RIVERA, R.J., GIUSTI, D. and ROSSI, R.: " Preliminary Geochemical and Thermodynamical Assessment of the St. Lucia (W.I.) Geothermal Resources at the Sulphur Springs Area", Applied Geochemistry, in press (1990).

10. D'AMORE, F. and PRUESS, K.:"Correlation between steam saturation, fluid composition and steam decline in vapor dominated reservoirs".Geothermics, vol. 15, n. 2, (1986), pp. 167-183.

11. D'AMORE, F. and GIANELLI, G: "Mineral assemblages and oxygen and sulphur fugacities in natural water-rock interaction processes". Geochim. et Cosmochim. Acta, vol. 49, (1984) pp. 847-857.

12. D'AMORE, F. and TRUESDELL, A.H.: "Calculation of geothermal reservoir temperatures and steam fraction from gas composition". Geothermal Resources Council Transactions, vol. 9, Part 1. (1985), pp. 305-310.

13. GIGGENBACH, W.F., GONFIANTINI, R., JANGI, B.L. and TRUESDELL, A.H.: "Isotopic and chemical composition of Parbati Valley geothermal discharges, NW Himalaya, India". Geothermics, vol. 12, n° 2/3, (1983), pp. 199-222.

14. CORSI, R.: "Scaling and Corrosion in geothermal equipment: problems and preventive measures". Geothermics, vol. 15, n° 5/6, (1986), pp. 839-856.

15. HAIZLIP, J.R. and TRUESDELL, A.H.: "Hydrogen Chloride in Superheated Steam at The Geysers Geothermal Field, California". Proc.13th Workshop Geothermal Res. Eng., Stanford University, (1988), pp. 93-100.

16. EARLOUGHER, R.C.,Jr.: "Advances in well test analysis", monography volume 5, Henry L. Doherty Series, SPE of AIME. Dallas, TEX (1977).

17. ECONOMIDES, M.J.: "Shut-in and Flowing Bottom-hole Pressure Calculation for Geothermal Steam Wells". Proc. Fifth Workshop on Geoth. Res. Eng., Stanford U., Stanford Ca. (Dec. 12-14, 1979).127-138.

18. RIVERA, R.J. and RAMEY, H.J., Jr. : "Application of two-rate flow tests to the determination of geothermal reservoir parameters", paper SPE 6887, presented at SPE-AIME 52nd Annual Technical

Conference, Denver, Colorado, Oct. 9-12, 1977.

19. CINCO-L., H.C., BRIGHAM, W.E., ECONOMIDES, M., MILLER, F.G., RAMEY, H.J., Jr., BARELLI, A. and MANETTI, G.,:"A Parallelepiped Model To Analize the Pressure Behaviour of Geothermal Steam Wells Penetrating Vertical Fractures", Paper SPE 8281, presented at the 54th Annual Fall Technical Conference and Exhibition, Soc. Pet.Eng. (1979).

20. AL-YOUSEF, H.Y.: "Limitations of the $\Delta p/q$ Approximation in the Analysis of Pressure Drawdown Interference with Variable Flow Rate", M Sc Report, Stanford U. (June, 1979).

21. BARELLI, A., BRIGHAM, W.E., CINCO-L., H., ECONOMIDES, M.J., MILLER, F.G., RAMEY, H.J., Jr, and SCHULTZ, A.: "Pressure Drawdown Analysis for the Travale - 22 Well", Proc. Fourth Workshop on Geoth. Res.Eng., Stanford U.(Dec., 1978) 165-175.

Table 1 - Summary of production data from the horizontal discharge test

Parameter Measured	Range	Observations
Total mass flow rate	24.8 - 47.5(ton.h)	
Liquid flow rate	0 - 9 (ton/h)	Liquid production ceased ceased at approx. 48h
Steam flow rate	15.9 - 35.2(ton/h)	
Gas flow rate	2.8 - 6.2 (ton/h)	CO_2: 90%, H_2S : 2.5%, (H_2 + CH_4 + N_2): 7.5%
Wellhead temperature	257 - 263°C	
Wellhead pressure	46.3 - 53.2 bar	
Water at weir box	pH : 4.5 - 7.5 Cl^-: 3000-15000ppm	
Enthalpy	2035 - 2669(Kj/Kg)	

Table 2 - Most representative gas composition (Vol.%)

CO_2	H_2S	H_2	CH_4	$COx10^4$	O_2x10^4	N_2	$Hex10^4$	$Arx10^4$
91.0 ±0.5	2.0 ±0.1	5.4 ±0.1	0.7 ±0.05	300 ±40	0.0	1.1 ±0.10	16+41	8+21

Table 3 - Isotopic analyses results of water and gas samples.

PRODUCING TIME h	δD (H_2O) °/.. vs SMOW	$\delta^{18}O$ (H_2O) °/.. vs SMOW	$\delta D(N_2)$ °/.. vs SMOW	$\delta D(CH_4)$ °/.. vs SMOW	$\delta^{13}C(CH_4)$ °/.. vs SMOW	$\delta^{13}C(CO_2)$ °/.. vs PDB
28.8 (1)	-23.5	+ 4.2				
70.3 (1)	-22.6	+ 5.3				
121.4 (1)	-25.0	+ 6.1				
28.8 (2)						-2.5
121.4 (2)			-414.3	-166.1	-21.4	-2.8

(1) total fluid sample
(2) dry gas sample

Table 4 - Condensed steam analyses (mg/l).

PRODUCING TIME h	pH	Temp °C	Cond. µS/cm	Alk. as $CaCO_3$	Ca	Mg	Na
3.0 (1)	6.0	20	355	100	2.1	0.02	2.0
69.0 (1)	5.7	20	445	148	2.6	0.04	1.6
28.8 (2)	5.48	20	625	223	0.7	<0.007	0.2
70.3 (2)	4.48	20	615	35	0.4	<0.007	0.1
126.0 (2)	2.68	20	1570	<1	<0.05	<0.007	0.02

1) Samples from initial discharge test
2) Samples from short-term production test

PRODUCING TIME h	K	Fe	Cl	H_2S	SiO_2	F	H_3BO_3	NH_4
3.0 (1)	1.4	0.41	9		0.72	<0.1	4.2	52
69.0 (1)	1.3	0.12	13		0.80	<0.1	26.9	72
28.8 (2)	0.1	0.13	6		0.08	1.2	297	106
70.3 (2)	0.08	3.9	139	106	0.14	1.3	498	82
126.0 (2)	<0.04	66	299	108	0.71	<0.1	606	74

1) Samples from initial discharge test
2) Samples from short-term production test

Table 5 -- Summary of results obtained from interpretation of pressure data from the short-term production test by means of several models.

PARAMETER	BUILDUP TEST		DRAWDOWN TEST		
	VARIABLE	HORNER	VARIABLE	PARALLELEPIPED	VERTICAL FRACTURE
kh(md.m)	3321	3690	3134	5280	2285
s	- 1.5	- 1.1.	-4.5	-	-
h (m)	-	-	-	208	$2 x_f h = 72321$
x_f (m)	-	-	-	29.7	

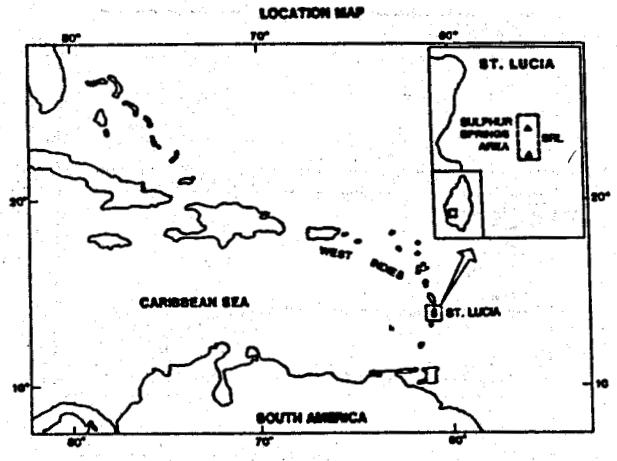

Fig. 1 Location of the geothermal resource.

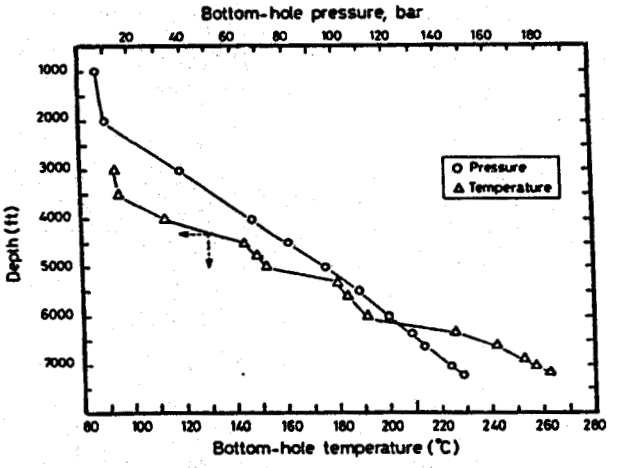

Fig. 3 P/T profiles from well SL-1.

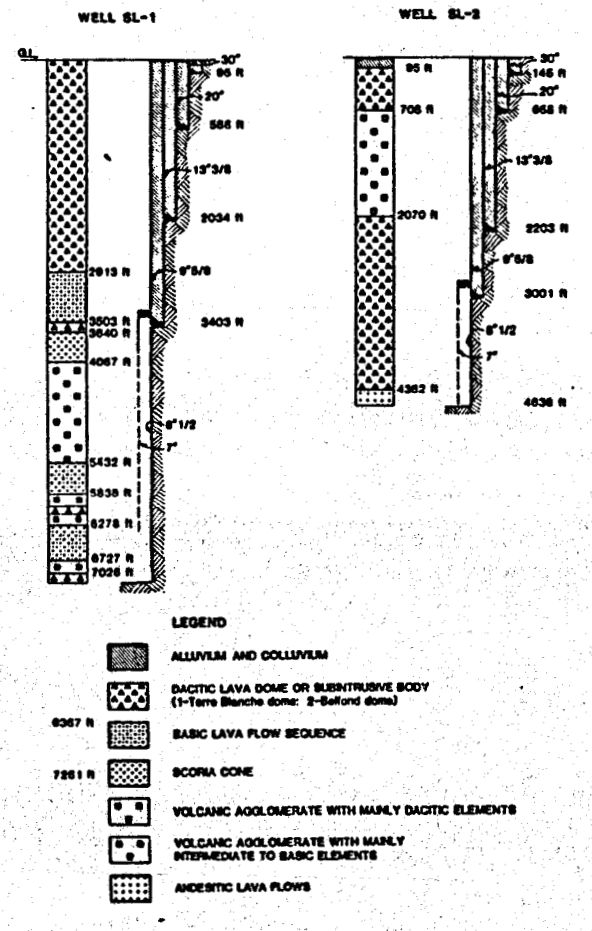

Fig. 2 Lithology and well completion of wells SL-1 and SL-2.

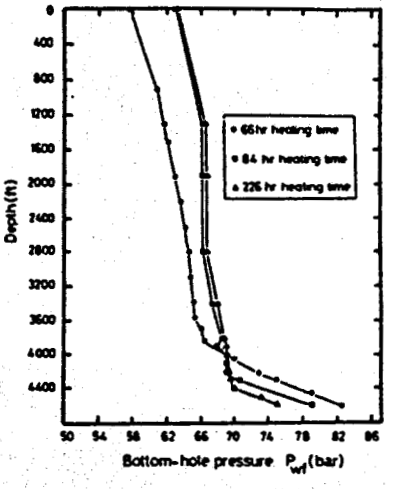

Fig. 4 Pressure profiles during warming-up well SL-2.

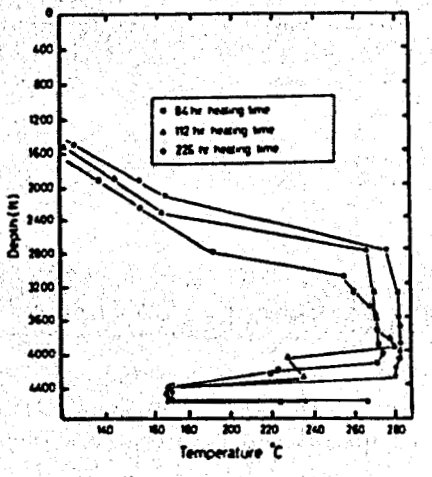

Fig. 5 Temperature profiles during warming-up of well SL-2.

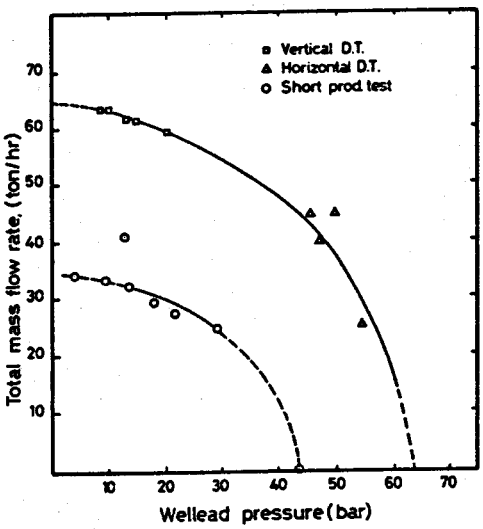

Fig. 6 Characteristic production curves of well SL-2 during the two production tests.

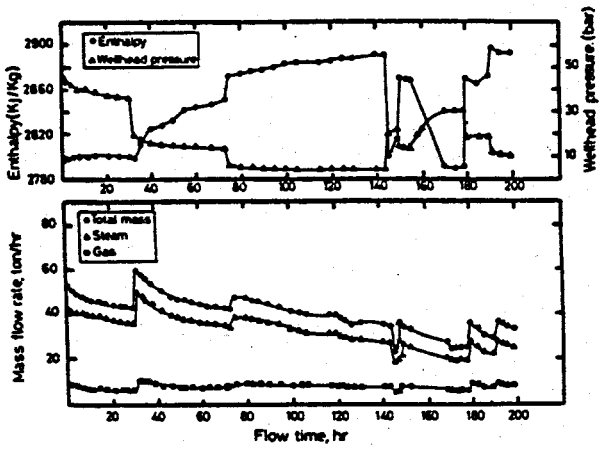

Fig. 7 Production data from the short-term test.

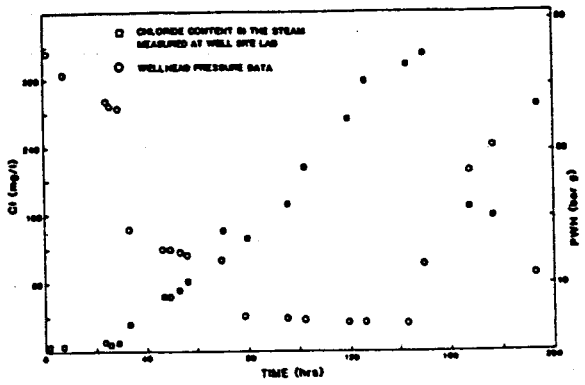

Fig. 8 Chloride content in the steam as a function of production time.

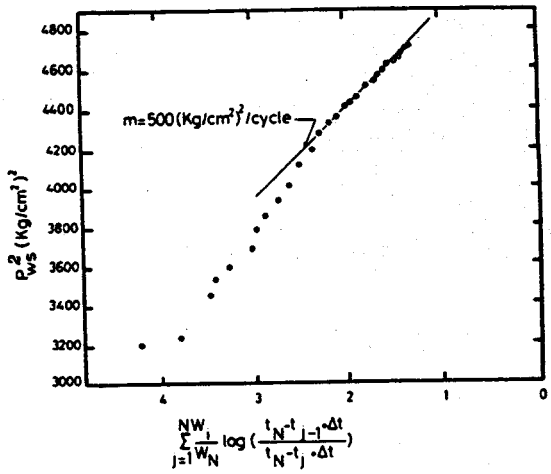

Fig. 9 Interpretation of buildup test with a variable flow rate history prior to shut-in.

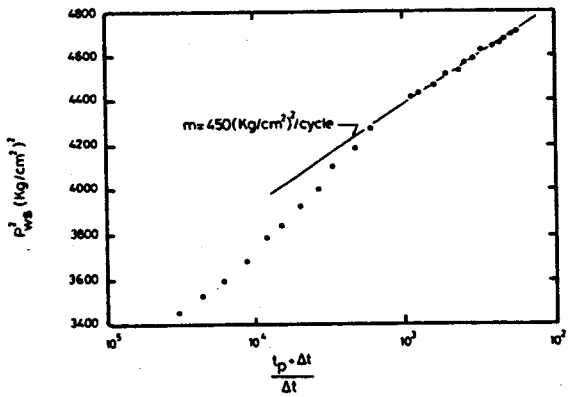

Fig. 10 Interpretation of buildup test by means of Horner model.

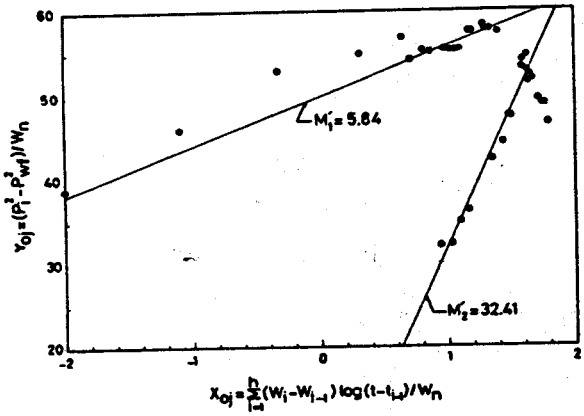

Fig. 11 Multiple-rate drawdown test during the horizontal discharge test (H.D.T.)

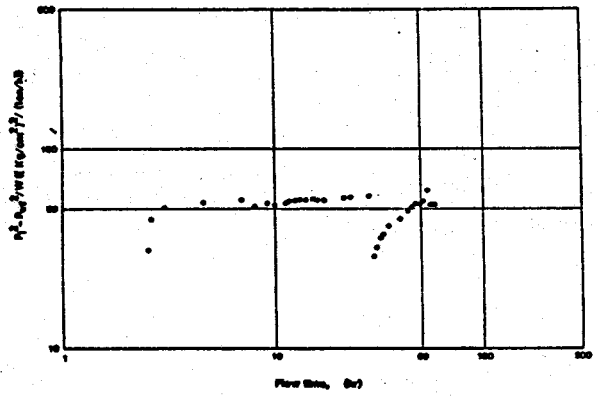

Fig. 12 Influence function vs. flow time for drawdown, H.D.T.

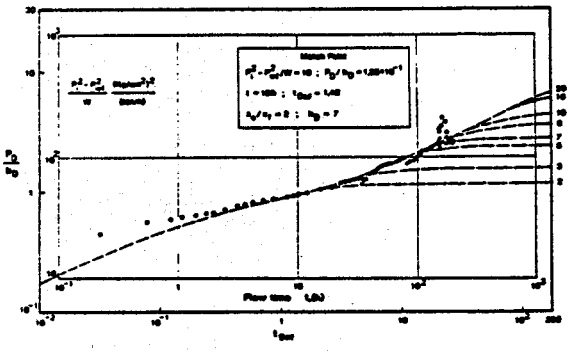

Fig. 14 Matching of drawdown data with the parallelepiped mode, S.T.P.T.

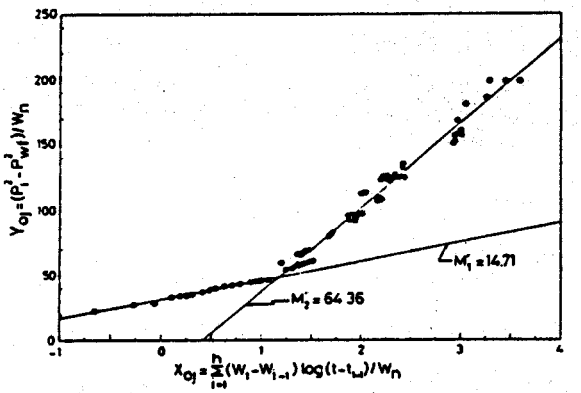

Fig. 13 Matching of drawdown test, short-term production test(S.T.P.T.).

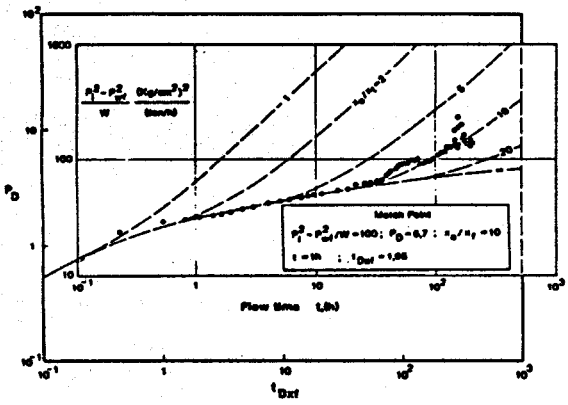

Fig. 15 Matching of drawdown data with the vertical fractured well, uniform-flux fracture, S.T.P.T.

CONCEPTUAL MODEL OF SULPHUR SPRINGS GEOTHERMAL AREA

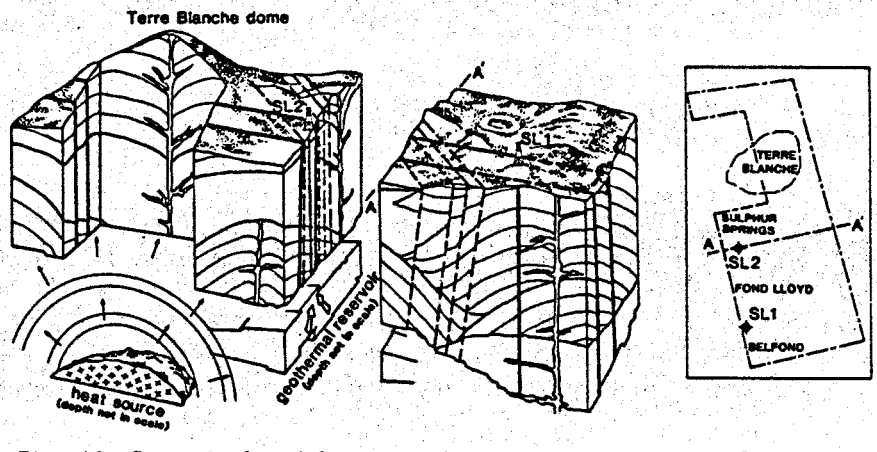

Fig. 16 Conceptual model of the Sulphur Springs geothermal resource.